energies

MDPI

Communication

Analysis of Electromagnetic–Mechanical Characteristics according to Shaft Materials of Permanent Magnet Synchronous Motor

Jeong-In Lee [1], Young-Cheol Kim [2], Jang-Young Choi [3] and Han-Wook Cho [4,*]

[1] Electric Power System Design Team, Hyundai Transys, Hwaseong-si 18603, Korea
[2] Department of System Dynamics, Korea Institute of Machinery and Materials, Daejeon 34103, Korea
[3] Department of Electrical Engineering, Chungnam National University, Daejeon 34134, Korea
[4] Department of Electrical, Electronic and Communication Engineering Education, Chungnam National University, Daejeon 34134, Korea
* Correspondence: hwcho@cnu.ac.kr

Abstract: In this paper, an analysis of electromagnetic–mechanical characteristics according to the shaft materials of a permanent magnet synchronous motor was performed. In general, the shaft of an electric motor rotating at high speed uses various materials, considering the mechanical rigidity and electromagnetic characteristics. However, because the material of the shaft has a significant influence on the electromagnetic performance according to the characteristics of the non-magnetic and magnetic materials, electromagnetic characteristics analysis was performed according to the material of the shaft. In addition, because the machine rotating at a high speed entails mechanical problems owing to the centrifugal force, the mechanical stability was secured through critical speed characteristic analysis according to each material after performing the von Mises stress analysis of the permanent magnet and sleeve.

Keywords: permanent magnet synchronous motor; shaft materials; electromagnetic–mechanical characteristics; synchronous inductance

Citation: Lee, J.-I.; Kim, Y.-C.; Choi, J.-Y.; Cho, H.-W. Analysis of Electromagnetic–Mechanical Characteristics according to Shaft Materials of Permanent Magnet Synchronous Motor. *Energies* **2022**, *15*, 8046. https://doi.org/10.3390/en15218046

Academic Editors: Yongxiang Xu and Guodong Yu

Received: 13 October 2022
Accepted: 27 October 2022
Published: 29 October 2022

1. Introduction

Owing to the advancement of manufacturing technology, electric motors using a permanent magnet with a high magnetic flux density have been used in various fields [1–8]. In particular, high-speed rotating machines using permanent magnets can afford high power density, system miniaturization, and efficiency by removing the gear box from the high-speed system using the existing induction machine and gear box [9–12]. In addition, as a gear box is not used, maintenance costs can be reduced, and due to various advantages, they are being applied in various industrial fields, such as compressors, pumps, and generators, and active research is still in progress [13–16]. However, as the rotational speed of the machines increases, various problems, such as an increase in iron loss due to high frequency, scattering of the rotor, and vibration and noise due to the resonant frequency, become issues, so design techniques considering these issues are being studied [17]. As the motor designed in this study rotates at a high speed of 28,000 rpm, various design methods were considered to satisfy the electromagnetic and mechanical properties, and lubrication-free magnetic bearings were used. Conventional mechanical bearings generate mechanical stress and heat due to physical contact.

Therefore, bearing damage and mechanical problems occur, resulting in reduced efficiency and system problems. To overcome these shortcomings, we recently checked the literature on the application of magnetic bearings to high-speed machines and used them in this study to eliminate mechanical contact. In this study, a heat-pump motor that operates under high-speed operating conditions and a high temperature difference

of over 70 °C. In general, machines rotating at high speeds have the advantage of system miniaturization and reduction of manufacturing costs owing to the direct-drive system that operates by directly coupling the load to the shaft [18,19]. However, as it rotates at high speed, mechanical problems arise due to centrifugal force development [20]. Therefore, for high-speed rotating machines, it is essential to perform rotor stress analysis and dynamics analysis [21]. Nevertheless, high-speed machines consist of materials with good mechanical rigidity as the shaft material of the rotating body in order to prevent various structural problems [22,23]. However, because the characteristics of the shaft material greatly affect the electromagnetic and mechanical properties of high-speed motors, it is necessary to analyze the detailed characteristics of permanent magnet motors [24,25].

Therefore, in this paper, after modeling the three-dimensional shape of a rotor, as shown in Figure 1, the electromagnetic–mechanical characteristics of the permanent magnet-type synchronous motor were analyzed for two shaft materials and a detailed comparison was performed using finite element analysis. The selected shaft materials were SCM440, which is generally inexpensive and widely used, and titanium (Ti-6AI-4V), which has excellent mechanical rigidity.

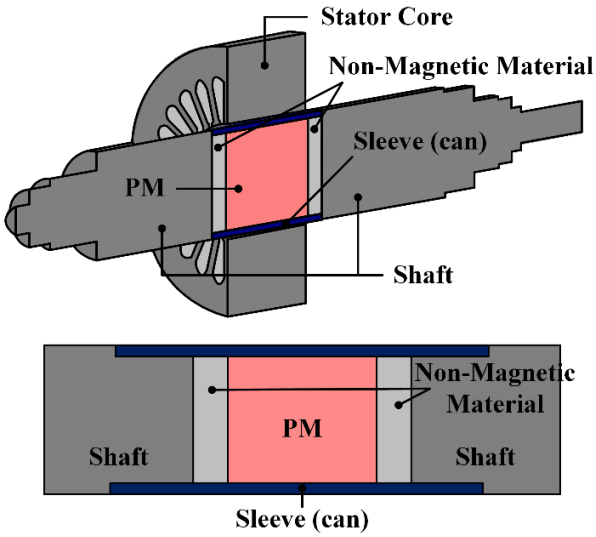

Figure 1. Structure of a permanent magnet motor.

Table 1 lists the requirements for the motor designed in this study. A permanent magnet synchronous motor was designed considering these requirements. The rotor size was limited to 85 mm and the operating temperature was 100 °C, which is considered a high operating temperature. Therefore, samarium cobalt (Sm_2Co_{17}) with high magnetic energy and good temperature characteristics was selected as the permanent magnet material, and the selected current density, based on the water cooling method, was approximately 10–12 A/mm^2.

Table 1. Design requirements.

Parameters	Value	Unit
Rated power	145	kW
Rated speed	28,000	rpm
Current density	10–12	A/mm^2
Operation temperature	100	°C
Outer diameter of rotor	85	mm
Line-to-line back-EMF	330	V_{rms}

2. Comparison of Electromagnetic Characteristics according to Shaft Materials

After designing the motor considering the above requirements, the electromagnetic characteristics of the motor according to the shaft material were analyzed using finite element analysis. First, because the line-to-line back-EMF of the motor has a limiting value of 330 V_{rms}, it was designed to not exceed this value. As shown in Figure 2, it was verified that the line-to-line back-EMF value did not exceed the limiting value. Subsequently, the inductance characteristics of the two types of motors were analyzed. Inductance represents the number of magnetic flux linkages per unit current and is a circuit constant that affects various electromagnetic characteristics, such as the power factor and efficiency of a device. The synchronous inductance analysis results are shown in Table 2, where the SCM440 material's inductance resistance was approximately 192.95 μH, while the titanium material had an inductance value of approximately 155.11 μH.

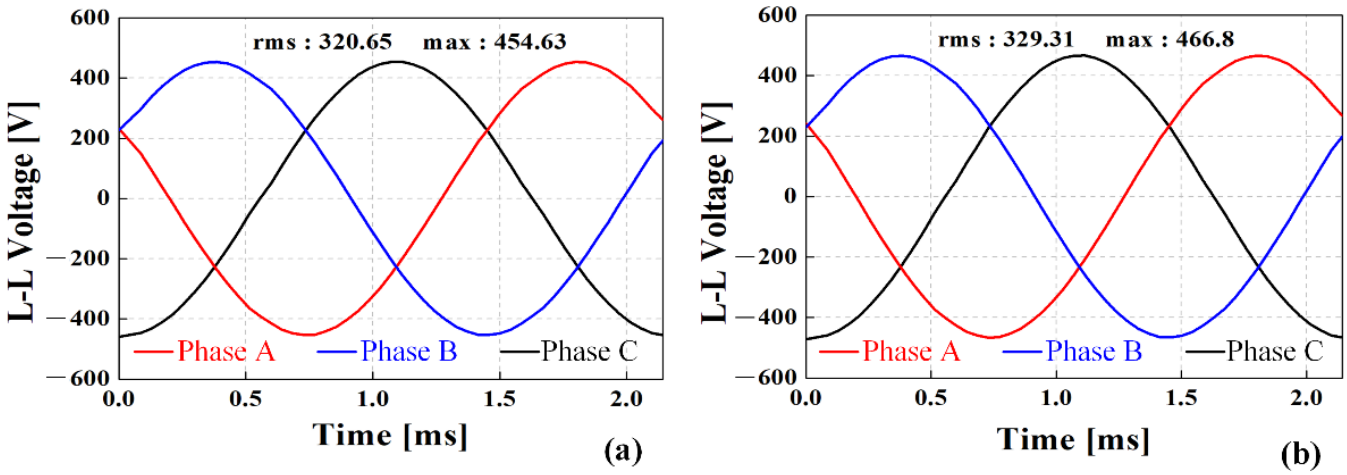

Figure 2. Line-to-line back-EMF at no-load according to shaft materials: (**a**) SCM440 shaft and (**b**) titanium shaft.

Table 2. Inductance characteristics according to the shaft materials.

Parameters	SCM440	Titanium
Self-inductance (μH)	157.03	131.56
Mutual inductance (μH)	35.92	23.55
Synchronous inductance (μH)	192.95	155.11

Thus, the motor inductance when using the SCM440 material was higher. The root cause for this difference in inductance values was analyzed, as shown in Figure 3. The results show that the magnetic flux leakage from the shaft was higher in the case of the SCM440 material. The titanium material had superior rigidity compared with the SCM440 material, and it had non-magnetic properties; therefore, leakage flux to the shaft did not occur significantly.

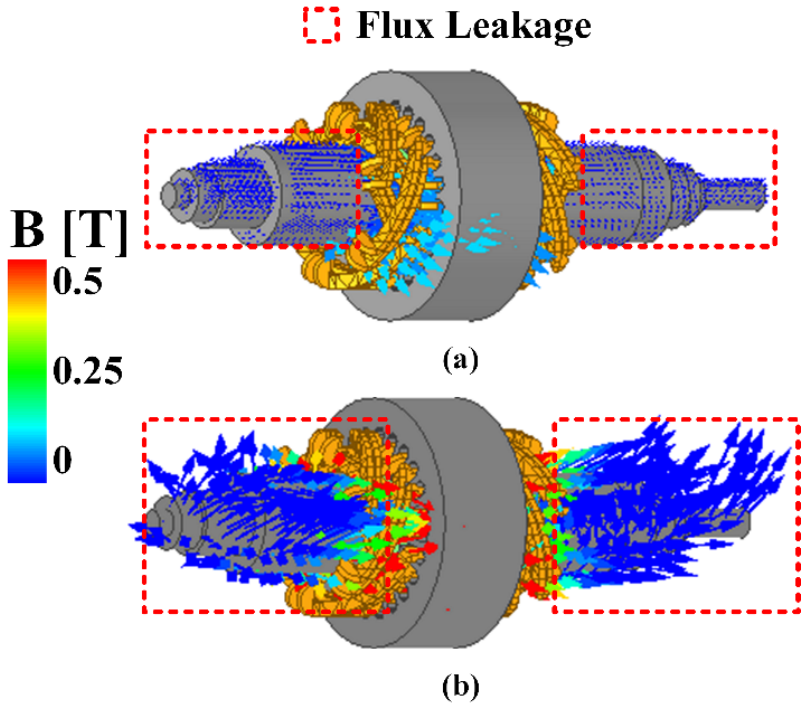

Figure 3. Leakage flux analysis results according to shaft materials: (**a**) titanium shaft and (**b**) SCM440 shaft.

However, in the case of SCM440, a large leakage flux occurred due to its magnetic properties. Magnetic flux leaking from the shaft increases the synchronous reactance component of a motor, which, in turn, may cause a voltage drop across the motor, leading to unsatisfactory results [24,26]. Therefore, load analysis of the motor was performed considering the magnetic flux leaking from the shaft and the end turn. A comparison of the characteristic analysis results under load conditions is presented in Table 3.

Table 3. Characteristic results at load according to shaft materials.

Parameters	SCM440	Titanium
Output power (kW)	145.1	145.7
Current (A_{rms})	270	260
Torque (Nm)	49.5	49.7
Core loss (W)	858.3	790.2
Eddy current loss (W)	298.8	289.6
Copper loss (kW)	1.95	1.81
Current density (A/mm^2)	9.76	9.4
Efficiency (%)	97.9	98.05

As a result of comparing the load characteristics, both motor types satisfied the requirements. Therefore, to confirm the operating range of the designed motor, the driving performance characteristics were analyzed according to the speed and torque of the two types of motors, as shown in Figures 4 and 5. First, in the case of the SCM440 material, the performance satisfied the requirements as a result of the analysis of the driving performance characteristics; however, there was little leeway as it spanned the operable range, as shown in Figure 4. In addition, the d-axis current required was approximately −167 A or greater, and the power factor was 87.4%, resulting in a relatively low result.

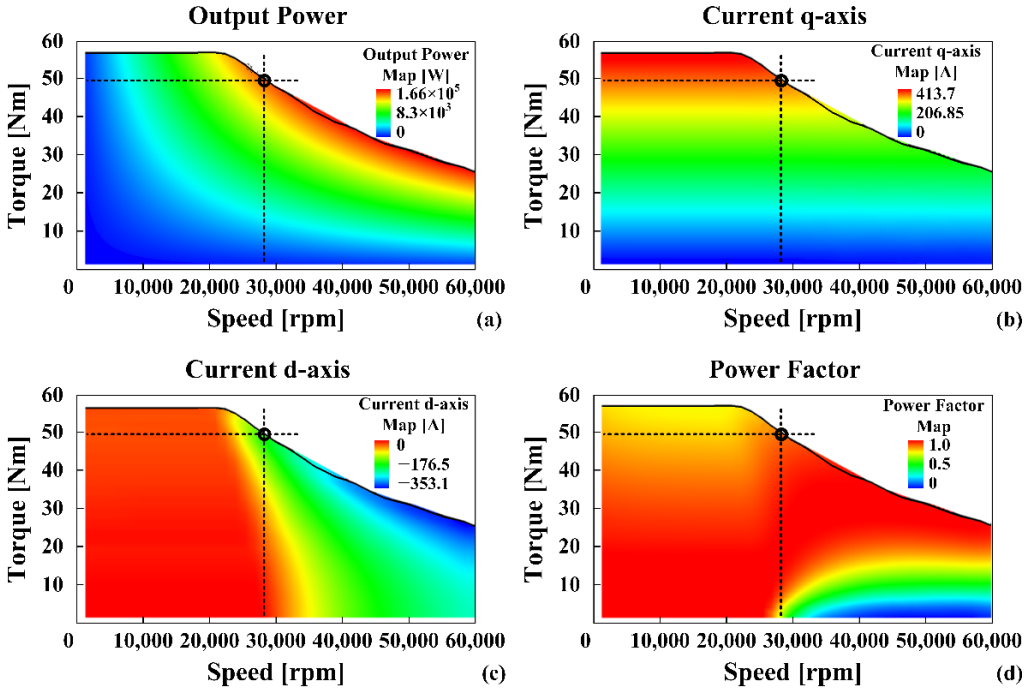

Figure 4. Operating performance results of SMC440 material shaft motor: (**a**) output power, (**b**) iq, (**c**) id, and (**d**) power factor.

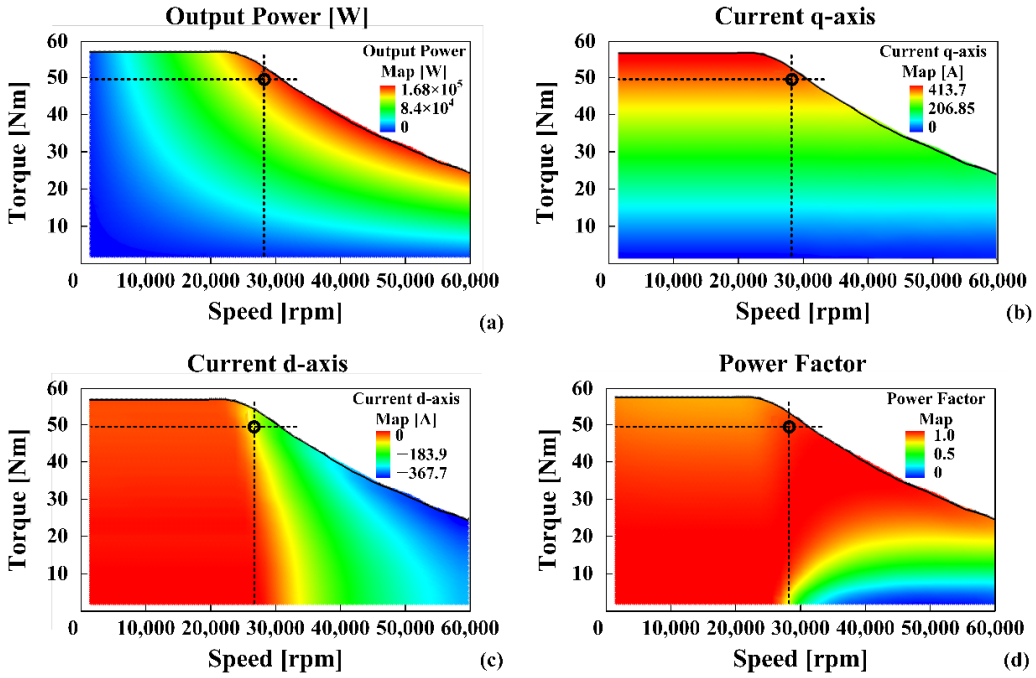

Figure 5. Operating performance results of titanium material shaft motor: (**a**) output power, (**b**) iq, (**c**) id, and (**d**) power factor.

The analysis of the performance characteristics of the motor using titanium material showed that it satisfied the requirements, as shown in Figure 5, and the operable range was wider than that of SCM440. The d-axis required was approximately −85 A or greater, and the power factor was greatly improved to approximately 91.6%. Table 4 lists the mechanical properties and cost of each material.

Table 4. Mechanical properties of the shaft materials.

Materials	Yield Strength (MPa)	Poisson's Ratio	Cost (kg/USD)
SCM440	830	0.284	2.71
Titanium	1100	0.33	38.46

In the case of the SCM440 material, the price is very low. However, the magnetic properties result in significant magnetic flux leakage, and the electromagnetic performance deteriorates. Conversely, the titanium material exhibits non-magnetic properties, resulting in favorable electromagnetic properties and excellent rigidity, but has a high price disadvantage. Designers must weigh these factors and consider this when designing.

3. Comparison of Mechanical Characteristics according to Shaft Materials

High-speed rotating permanent magnet machines require a sleeve to prevent the magnet from breaking and scattering due to centrifugal forces [25,27–29]. In general, the sleeve uses a nonmagnetic material and is integrated with a permanent magnet through a shrink fit [30–32]. As a result, mechanical stress occurs between the permanent magnet and sleeve, and mechanical stress arises due to centrifugal forces associated with high-speed rotating objects. Rotor damage is caused when the stress generated inside the rotor exceeds the yield stress of the material of each rotor, leading to system failure. Therefore, to prevent damage to the rotor, the mechanical stress caused by high-speed rotation and the structural response to the natural frequency must be considered in the initial design stage of the machines [33,34]. Therefore, in this chapter, mechanical characteristic analysis of the designed motor is performed.

Figure 6 shows the von Mises stress analysis results for the design model. The von Mises stress analysis was performed on the permanent magnet and sleeve area of the rotor.

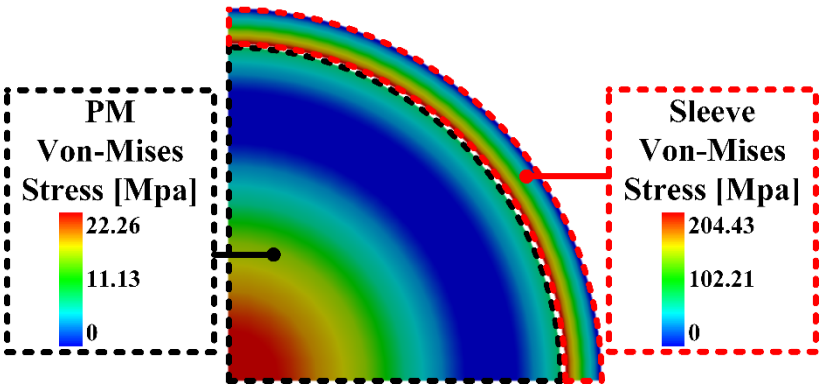

Figure 6. Analysis result of rotor von Mises stress.

For permanent magnets, Sm_2Co_{17} material with good temperature characteristics was used. The sleeve material had non-magnetic characteristics, and the same titanium material as the shaft was used. The mechanical properties of each rotor material are listed in Table 5, and the results of the characteristic analysis showed that the yield stress did not deviate when a mechanical safety factor of 1.5 was considered for both the permanent magnet and sleeve. Therefore, the structural stability of the designed rotor was confirmed. After that, in order to satisfy the requirements and determine the margin of operation, a frequency response function (FRF) experiment of the rotating body was performed in consideration of the impeller after manufacturing a rotor from titanium material with excellent electromagnetic characteristics.

Table 5. Mechanical properties of permanent magnet and sleeve materials.

Parameters \ Materials	Sleeve Titanium	PM Sm_2Co_{17}
Density (kg/m^3)	4430	8400
Poisson's ratio	0.33	0.24
Young's modulus (Gpa)	1.14	120
Yield strength (MPa)	1100	35

The FRF experiment produced a Free–Free state by fixing the rotor with thin straps at both ends so that the rotor could remain as free as possible. Additionally, tuning was performed to avoid the natural frequency using an impact hammer. The mode test was performed at three locations on the rotating body.

The first bending mode derived through the experiment was approximately located at 589 Hz, and the second mode was approximately located at 1060 Hz. The experimental characteristics results and the shape of the rotor (PM, sleeve, and shaft) are shown in Figure 7. The reason why the double peak appeared as a result of the analysis was that the axis was slightly anisotropically fixed in the vertical direction. Therefore, a double peak occurred. Additionally, the reason that the peak size was different for each location was because the response magnitude of each vibration mode was different for each location. Next, critical speed characteristic analysis of the rotor was performed to confirm the validity of the FRF experiment. High-speed machines generate various natural frequencies owing to their high rotational speeds, which lead to damaged bearings and systems. Therefore, dynamic analysis of a rotating body is essential [35–37]. In a high-speed rotating machine, rigid and bending modes occur in a rotating body. When operating in the same area where rigid and bending modes occur, rotor damage and deformation can occur due to the natural frequency. To prevent this from occurring, a critical speed analysis was performed, as shown in Figure 8. Each color line means rigid and bending mode according to each order. As the rated speed of the designed motor was at the level of 28,000 rpm, the maximum rotational speed was increased up to the level of 100,000 rpm when analyzing the critical speed.

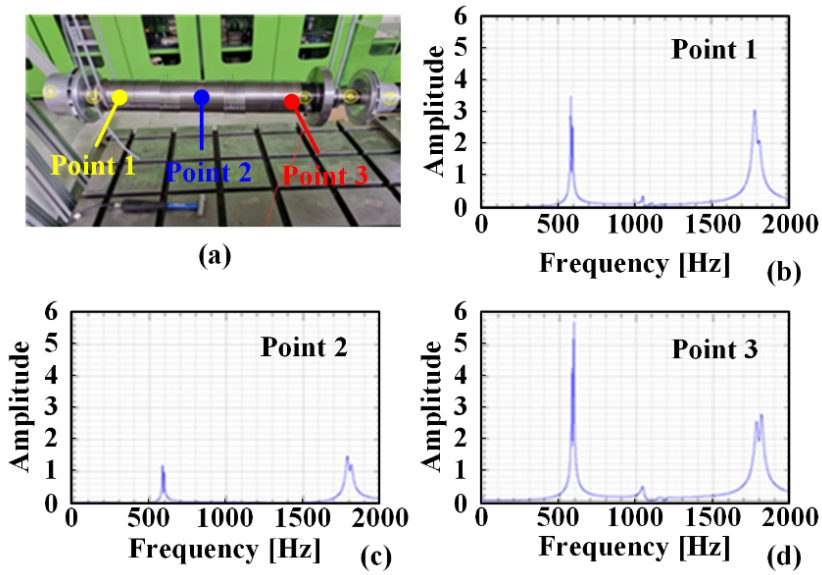

Figure 7. FRF experiment results of the rotating body: (**a**) experimental model, (**b**) point 1 test, (**c**) point 2 test, and (**d**) point 3 test.

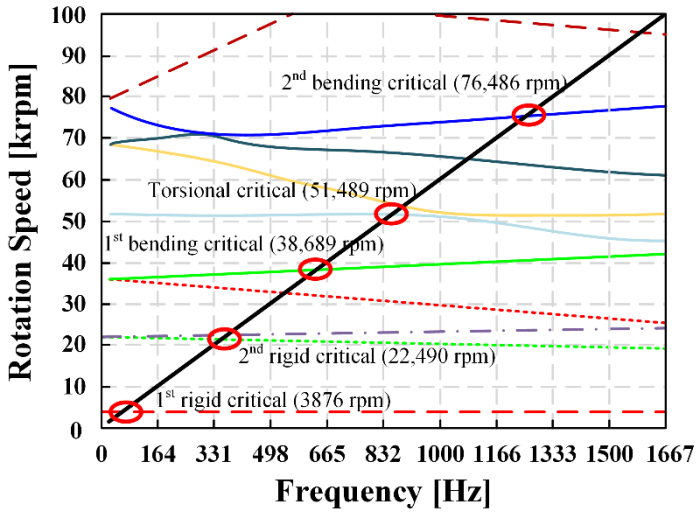

Figure 8. Analysis results of the critical speed characteristic.

In the first and second rigid modes, the operating speeds were 3876 rpm and 22,490 rpm, respectively. As the rated rotation speed was 28,000 rpm, the second rigid body mode had a margin of approximately 20%. It was confirmed that the first and second bending speeds were 38,689 rpm and 76,486 rpm, respectively, with a margin of approximately 38% at this rated speed. In addition, the torsional critical operation speed was 51,489 rpm, and it was considered that there was no mechanical problem because the point that intersected with the natural frequency point of the designed rotating body did not occur.

4. Conclusions

In this study, design and analysis were performed to satisfy the electromagnetic–mechanical characteristics related to the shaft material of a permanent magnet synchronous motor. The design specifications of the final designed permanent magnet synchronous motor are shown in Table 6. For the shaft material, two materials, SCM440, which is generally inexpensive, and titanium, which has non-magnetic properties, were used. In the case of SCM440, it had the advantage of reducing the manufacturing cost because the price was very low, but it was confirmed that there was no leeway for the power factor and operating performance range when compared with the titanium material. On the other hand, the non-magnetic properties of titanium resulted in a small magnetic flux leakage, so the power factor and operating performance range were advantageous compared with SCM440. However, titanium costs approximately 14 times the cost of SCM440, which can result in high manufacturing costs.

Table 6. Final design specification.

Parameters	Value	Unit
Outer diameter of stator	210	mm
Outer diameter of rotor	85	mm
Thickness of sleeve	4	mm
Air gap length	1.8	mm
Axial length	84	mm

Subsequently, rotor stress and critical speed analysis were performed in relation to the high-speed rotation conditions of the designed motor. As a result of the stress analysis, it was confirmed that a safety factor of 1.5 was taken into consideration at the rated speed and mechanically stable. In addition, through a critical speed analysis, it was confirmed that the critical speed of the rotating body did not match the rated speed, and the validity was verified through experiments on the manufactured rotating body. Therefore, through this

study, it was confirmed that the electromagnetic and mechanical properties of the machine had a large effect, depending on the shaft material, and it was considered to be sufficiently applicable to various permanent magnet devices. In addition, when using the SCM440 material for a shaft, it has the advantage of low manufacturing cost, and when excellent electromagnetic performance is required, it is advantageous to use a non-magnetic titanium material. Therefore, a designer should take this into consideration when designing.

Author Contributions: J.-I.L., writing—original draft preparation, formal analysis, and validation; Y.-C.K., formal analysis and validation; J.-Y.C., writing—review and editing; H.-W.C., writing—review and editing, and validation. All authors have read and agreed to the published version of the manuscript.

Funding: This work was supported by the Technology Innovation Program funded By the Ministry of Trade, Industry and Energy (MOTIE, Korea) under Grant 20010090.

Data Availability Statement: Not applicable.

Conflicts of Interest: The authors declare no conflict of interest.

References

1. Jing, L.; Tang, W.; Wang, T.; Ben, T.; Qu, R. Performance Analysis of Magnetically Geared Permanent Magnet Brushless Motor for Hybrid Electric Vehicles. *IEEE Trans. Transp. Electrif.* **2022**, *8*, 2874–2883. [CrossRef]
2. Paul, S.; Chang, J. Fast Model-Based Design of High Performance Permanent Magnet Machine for Next Generation Electric Propulsion for Urban Aerial Vehicle Application. *CES Trans. Electr. Mach. Syst.* **2021**, *5*, 143–151. [CrossRef]
3. Lee, Y.H.; Hsieh, M.F.; Chen, P.H. A Novel Variable Flux Spoke Type Permanent Magnet Motor with Swiveling Magnetization for Electric Vehicles. *IEEE Access* **2022**, *10*, 62194–62209. [CrossRef]
4. Mahmouditabar, F.; Vahedi, A.; Takorabet, N. Design and Analysis of Interior Permanent Magnet Motor for Electric Vehicle Application Considering Irreversible Demagnetization. *IEEE Trans. Ind. Appl.* **2022**, *58*, 284–293. [CrossRef]
5. Sun, X.; Shi, Z.; Cai, Y.; Lei, G.; Guo, Y.; Zhu, J. Driving-Cycle-Oriented Design Optimization of a Permanent Magnet Hub Motor Drive System for a Four-Wheel-Drive Electric Vehicle. *IEEE Trans. Transp. Electrif.* **2020**, *6*, 1115–1125. [CrossRef]
6. Li, W.; Cao, Z.; Zhang, X. Thermal Analysis of the Solid Rotor Permanent Magnet Synchronous Motors With Air-Cooled Hybrid Ventilation Systems. *IEEE Trans. Ind. Electron.* **2022**, *69*, 1146–1156. [CrossRef]
7. Xu, Y.; Ai, M.; Xu, Z.; Liu, W.; Wang, Y. Research On Interior Permanent Magnet Synchronous Motor Based on Performance Matching of Electric Bus. *IEEE Trans. Appl. Supercond.* **2021**, *31*, 5204304. [CrossRef]
8. Tak, B.-O.; Ro, J.-S. Analysis and Design of an Axial Flux Permanent Magnet Motor for in-Wheel System Using a Novel Analytical Method Combined With a Numerical Method. *IEEE Access* **2020**, *8*, 203994–204011. [CrossRef]
9. Dong, B.; Wang, K.; Han, B.; Zheng, S. Thermal Analysis and Experimental Validation of a 30 kW 60000 r/min High-Speed Permanent Magnet Motor With Magnetic Bearings. *IEEE Access* **2019**, *7*, 92184–92192. [CrossRef]
10. Zhang, C.; Chen, L.; Wang, X.; Tang, R. Loss Calculation and Thermal Analysis for High-Speed Permanent Magnet Synchronous Machines. *IEEE Access* **2020**, *8*, 92627–92636. [CrossRef]
11. Liu, Z.; Chiba, A.; Irino, Y.; Nakazawa, Y. Optimum Pole Number Combination of a Buried Permanent Magnet Bearingless Motor and Test Results at an Output of 60 kW With a Speed of 37000 r/min. *IEEE Open J. Ind. Appl.* **2020**, *1*, 33–41. [CrossRef]
12. Cheng, X.; Xu, W.; Du, G.; Zeng, G.; Zhu, J. Novel rotors with low eddy current loss for high speed permanent magnet machines. *CES Trans. Electr. Mach. Syst.* **2019**, *3*, 187–194. [CrossRef]
13. Bhuiyan, N.A.; McDonald, A. Optimization of Offshore Direct Drive Wind Turbine Generator With Consideration of Permanent Magnet Grade and Temperature. *IEEE Trans. Energy Convers.* **2018**, *34*, 1105–1114. [CrossRef]
14. Gerada, D.; Huang, X.; Zhang, C.; Zhang, H.; Zhang, X.; Gerada, C. Electrical Machines for Automotive Electrically Assisted Turbocharging. *IEEE/ASME Trans. Mechatron.* **2018**, *23*, 2054–2065. [CrossRef]
15. Wu, S.; Tong, W.; Li, W.; Yu, S.; Tang, R. Electromagnetic Vibration Analysis of High-Speed Permanent Magnet Synchronous Machines With Amorphous Metal Stator Cores Considering Current Harmonics. *IEEE Trans. Ind. Electron.* **2020**, *67*, 10156–10167. [CrossRef]
16. Zhang, Z.; Deng, Z.; Sun, Q.; Peng, C.; Gu, Y.; Pang, G. Analytical Modeling and Experimental Validation of Rotor Harmonic Eddy-Current Loss in High-Speed Surface-Mounted Permanent Magnet Motors. *IEEE Trans. Magn.* **2019**, *55*, 8100811. [CrossRef]
17. Lee, J.-I.; Shin, K.-H.; Bang, T.-K.; Choi, B.-S.; Kim, B.-O.; Choi, J.-Y. Experiments and Design Criteria for a High-Speed Permanent Magnet Synchronous Generator With Magnetic Bearing Considering Mechanical Aspects. *IEEE Trans. Appl. Supercond.* **2020**, *30*, 5204205. [CrossRef]
18. Qiu, H.; Tang, B.; Yu, W.; Yuan, S.; Wu, J.; Yang, C.; Cui, G. Analysis of the super high-speed permanent magnet generator under unbalanced load condition. *IET Electr. Power Appl.* **2017**, *11*, 1492–1498. [CrossRef]
19. Zhang, Y.; McLoone, S.; Cao, W.; Qiu, F.; Gerada, C. Power Loss and Thermal Analysis of a MW High-Speed Permanent Magnet Synchronous Machine. *IEEE Trans. Energy Convers.* **2017**, *32*, 1468–1478. [CrossRef]

20. Jang, S.-M.; Ko, K.-J.; Cho, H.-W.; Choi, J.-Y. Electromechanical Parameters Calculation of Permanent Magnet Synchronous Motor Using the Transfer Relations Theorem. *IEEE Trans. Magn.* **2007**, *43*, 2495–2497. [CrossRef]
21. Ahn, J.-H.; Han, C.; Kim, C.-W.; Choi, J.-Y. Rotor Design of High-Speed Permanent Magnet Synchronous Motors Considering Rotor Magnet and Sleeve Materials. *IEEE Trans. Appl. Supercond.* **2018**, *28*, 5201504. [CrossRef]
22. Jang, G.-H.; Ahn, J.-H.; Kim, B.-O.; Lee, D.-H.; Bang, J.-S.; Choi, J.-Y. Design and Characteristic Analysis of a High-Speed Permanent Magnet Synchronous Motor Considering the Mechanical Structure for High-Speed and High-Head Centrifugal Pumps. *IEEE Trans. Magn.* **2018**, *54*, 8204906. [CrossRef]
23. Ou, J.; Liu, Y.; Breining, P.; Gietzelt, T.; Wunsch, T.; Doppelbauer, M. Experimental Characterization and Feasibility Study on High Mechanical Strength Electrical Steels for High-Speed Motors Application. *IEEE Trans. Ind. Appl.* **2021**, *57*, 284–293. [CrossRef]
24. Shin, K.-H.; Bang, T.-K.; Cho, H.-W.; Choi, J.-Y. Design and Analysis of High-Speed Permanent Magnet Synchronous Generator With Rotor Structure Considering Electromechanical Characteristics. *IEEE Trans. Appl. Supercond.* **2020**, *30*, 5204305. [CrossRef]
25. Lee, J.-I.; Bang, T.-K.; Lee, H.-K.; Woo, J.-H.; Nah, J.; Choi, J.-Y. Design of the High-Speed PMSG with Two Different Shaft Material Considering Overhang Effect and Mechanical Characteristics. *Appl. Sci.* **2021**, *11*, 7670. [CrossRef]
26. Shin, K.-H.; Jung, K.-H.; Cho, H.-W.; Choi, J.-Y. Analytical Modeling and Experimental Verification for Electromagnetic Analysis of Tubular Linear Synchronous Machines With Axially Magnetized Permanent Magnets and Flux-Passing Iron Poles. *IEEE Trans. Magn.* **2018**, *54*, 8204006. [CrossRef]
27. Zhang, F.; Du, G.; Wang, T.; Liu, G.; Cao, W. Rotor Retaining Sleeve Design for a 1.12-MW High-Speed PM Machine. *IEEE Trans. Ind. Appl.* **2015**, *51*, 3675–3685. [CrossRef]
28. Zheng, J.; Zhao, W.; Ji, J.; Zhu, J.; Lee, C.H.T. Sleeve design of permanent-magnet machine for low rotor losses. *IEEE Chinese Journal of Electrical Engineering.* **2020**, *6*, 86–96. [CrossRef]
29. Han, T.; Wang, Y.-C.; Shen, J.-X. Analysis and Experiment Method of Influence of Retaining Sleeve Structures and Materials on Rotor Eddy Current Loss in High-Speed PM Motors. *IEEE Trans. Ind. Appl.* **2020**, *56*, 4889–4895. [CrossRef]
30. Zhu, Z.; Huang, Y.; Dong, J.; Peng, F.; Yao, Y. Rotor Eddy Current Loss Reduction With Permeable Retaining Sleeve for Permanent Magnet Synchronous Machine. *IEEE Trans. Energy Convers.* **2020**, *35*, 1088–1097. [CrossRef]
31. Zhang, H.; Zhang, X.; Gerada, C.; Galea, M.; Gerada, D.; Li, J. Design Considerations for the Tooth Shoe Shape for High-Speed Permanent Magnet Generators. *IEEE Trans. Magn.* **2015**, *51*, 8112904. [CrossRef]
32. Woo, J.-H.; Bang, T.-K.; Kim, C.-W.; Yoon, I.-J.; Choi, J.-Y. Experimental and comparative study of mechanical and electromagnetic aspects of a high-speed permanent magnetic motor with two different magnetic materials. *AIP Adv.* **2020**, *10*, 015217. [CrossRef]
33. Cho, H.-W.; Ko, K.-J.; Choi, J.-Y.; Shin, H.-J.; Jang, S.-M. Rotor Natural Frequency in High-Speed Permanent-Magnet Synchronous Motor for Turbo-Compressor Application. *IEEE Trans. Magn.* **2011**, *47*, 4258–4261. [CrossRef]
34. Bang, T.-K.; Shin, K.-H.; Lee, J.-I.; Woo, J.-H.; Cho, H.-W.; Choi, J.-Y. Design of high-speed permanent magnet synchronous machines considering thermal demagnetization and mechanical characteristic of permanent magnet. *AIP Adv.* **2021**, *11*, 025129. [CrossRef]
35. Huang, Z.; Fang, J. Multiphysics Design and Optimization of High-Speed Permanent-Magnet Electrical Machines for Air Blower Applications. *IEEE Trans. Ind. Electron.* **2016**, *63*, 2766–2774. [CrossRef]
36. Fang, H.; Qu, R.; Li, J.; Zheng, P.; Fan, X. Rotor Design for High-Speed High-Power Permanent-Magnet Synchronous Machines. *IEEE Trans. Ind. Appl.* **2017**, *53*, 3411–3419. [CrossRef]
37. Ede, J.; Zhu, Z.; Howe, D. Rotor resonances of high-speed permanent-magnet brushless machines. *IEEE Trans. Ind. Appl.* **2002**, *38*, 1542–1548. [CrossRef]